Inorg. Chem. **2006**, *45*, 5867−5877

Reactivity of Lanthanocene Hydroxides toward Ketene, Isocyanate, Lanthanocene Alkyl, and Triscyclopentadienyllanthanide Complexes

Chunmei Zhang,[†] Ruiting Liu,[†] Jie Zhang,[†] Zhenxia Chen,[†] and Xigeng Zhou*[,†,‡]

Department of Chemistry, Molecular Catalysis and Innovative Material Laboratory, Fudan University, Shanghai 200433, People's Republic of China, and State Key Laboratory of Organometallic Chemistry, Shanghai 200032, People's Republic of China

Received February 21, 2006

The reactivity of $[Cp_2Ln(\mu\text{-}OH)(THF)]_2$ (Ln = Y (**1**), Er (**2**), Yb (**3**)) toward PhEtCCO, PhNCO, Cp_3Ln, $[Cp_2Ln(\mu\text{-}CH_3)]_2$, and the LiCl adduct of $Cp_2Ln^nBu(THF)_x$ was examined. In all cases, OH-centered reactivity is observed: complexes **1**–**3** react with PhEtCCO to form the O–H addition products $[Cp_2Ln(\mu\text{-}\eta^1\text{:}\eta^2\text{-}O_2CCHEtPh)]_2$ (Ln = Yb (**5**), Er (**6**), Y (**7**), respectively, for **1**–**3**), whereas treatment of **1** with PhNCO affords the addition/CpH-elimination/rearrangement product $[\{Cp_2Y(THF)\}_2(\mu\text{-}\eta^2\text{:}\eta^2\text{-}O_2CNPh)]$ (**8**), which contains an unusual $PhNCO_2$ dianionic ligand. Analogous compound $[Cp_2Ln(THF)]_2(\mu\text{-}\eta^2\text{:}\eta^2\text{-}O_2CNPh)$ (Ln = Yb (**9**), Er (**10**)) and **8** can be obtained in a higher yield by treatment of $[Cp_2Ln(\mu\text{-}OH)(THF)]_2$ with PhNCO followed by reaction with the corresponding Cp_3Ln. However, attempts to prepare the corresponding heterobimetallic complex by reacting stoichiometric amounts of $[Cp_2Y(\mu\text{-}OH)(THF)]_2$ with PhNCO followed by treating it with Cp_3Yb are unsuccessful. Instead, only rearrangement products **8** and **9** are obtained. Furthermore, the reaction of **3** with $[Cp_2Yb(\mu\text{-}CH_3)]_2$ or Cp_3Yb forms oxo-bridged compound $[Cp_2Yb(THF)]_2(\mu\text{-}O)$ (**11**), whereas the reaction of $[Cp_2ErCl]_2$ with Li^nBu followed by treatment with **2** affords unexpected μ-oxo lanthanocene cluster $(Cp_2Er)_3(\mu\text{-}OH)(\mu_3\text{-}O)(\mu\text{-}Cl)Li(THF)_4$ (**12**). In contrast to **1** and **2**, **3** shows a strong tendency to undergo the intermolecular elimination of CpH at room temperature, giving trinuclear species $[Cp_2Yb(\mu\text{-}OH)]_2[CpYb(THF)](\mu_3\text{-}O)$ (**4**). The single-crystal X-ray diffraction structures of **1**, **2**, and **4**–**12** are described. All the results offer an interesting contrast to transition- and main-metal hydroxide complexes.

Introduction

The ligand-based reaction of organometallic compounds is a valuable synthetic tool, because it allows for the introduction of alternate substituents onto ancillary ligands. Such a reaction has become a very powerful and efficient method for the synthesis of a wide variety of transition-metal organometallic derivatives, especially those that cannot be easily prepared by other synthetic methods.[1] In addition, this strategy is also very useful in organic transformations, such as transition-metal-mediated dearomatization reactions.[2,3] However, very few examples of ligand-based reactions of organolanthanides have been reported because of the facile cleavage of the original metal−ligand bonds under the reaction conditions involved, which makes it difficult to access potentially suitable reactants and control the selectivity.[4,5] This is unfortunate, because the rare earth elements represent the largest subgroup in the periodic table and offer

* To whom correspondence should be addressed. E-mail: xgzhou@fudan.edu.cn. Fax: 86 21-65641740. Phone: 86 21-65643769.

[†] Fudan University.

[‡] State Key Laboratory of Organometallic Chemistry.

(1) (a) Hayashi, T. In *Ferrocenes*; Togni, A., Hayashi, T., Eds.; VCH: Weinheim, Germany, 1995; pp 105−142. (b) Cardin, D. J.; Cetinkaya, B.; Lappert, M. F. *Chem. Rev.* **1972**, *72*, 545−574. (c) Chen, J.-T. *Coord. Chem. Rev.* **1999**, *192*, 1143−1168. (d) Cuenca, T.; Royo, P. *Coord. Chem. Rev.* **1999**, *195*, 447−498.

(2) (a) Bach, T. *Angew. Chem., Int. Ed.* **1996**, *35*, 729−730. (b) Pape, A. R.; Kaliapan, K. P.; Kündig, E. P. *Chem. Rev.* **2000**, *100*, 2917−2940. (c) Harman, W. D. *Chem. Rev.* **1997**, *97*, 1953−1978. (d) Harman, W. D. *Coord. Chem. Rev.* **2004**, *248*, 853−866. (e) Brooks, B. C.; Gunnoe, T. B.; Harman, W. D. *Coord. Chem. Rev.* **2000**, *206*, 3−61. (f) Berger, A.; Djukic, J.-P.; Michon, C. *Coord. Chem. Rev.* **2002**, *225*, 215−238. (g) Kündig, E. P. *Transition Metal Arene π Complexes in Organic Synthesis and Catalysis*; Springer-Verlag: Berlin, 2004.

(3) (a) Maruoka, K.; Ito, M.; Yamamoto, H. *J. Am. Chem. Soc.* **1995**, *117*, 9091−9092. (b) Barluenga, J.; Trabanco, A. A.; Flórez, J.; García-Granda, S.; Martín, E. *J. Am. Chem. Soc.* **1996**, *118*, 13099−13100.

(4) (a) Schumann, H.; Heim, A.; Demtschuk, J.; Mühle, S. H. *Organometallics* **2003**, *22*, 118−128. (b) Liu, Q. C.; Ding, M. X.; Lin, Y. H.; Xing, Y. *J. Organomet. Chem.* **1997**, *548*, 139−142.

(5) (a) Zhang, J.; Cai, R. F.; Weng, L. H.; Zhou, X. G. *Dalton Trans.* **2006**, 1168−1173. (b) Zhou, X. G.; Zhu, M.; Zhang, L. B.; Zhu, Z. Y.; Pi, C. F.; Pang, Z.; Weng, L. H.; Cai, R. F. *Chem. Commun.* **2005**, 2342−2344.

10.1021/ic0602998 CCC: $33.50
Published on Web 06/30/2006

a unique, gradual variation in the properties that can be important in optimizing and directing the reaction chemistry. In fact, the paucity of ligand-based reactions in lanthanide chemistry not only restricts the development of supported ligands but influences the evolution of lanthanide-based catalytic systems to a certain extent. Therefore, the design of novel ligand-based reactions is a highly desirable and challenging task in organolanthanide chemistry.

The selected transformation of the hydroxide ligand is very attractive in main- and transition-metal chemistry because of its relevance to industrial and biological processes.[6−10] However, to the best of our knowledge, there is essentially nothing known about the regioselective transformation of the OH ligand of organolanthanide hydroxides, despite the fact that they have been known for a long time.[11] Considering the strongly electrophilic and oxophilic character of rare earth elements, it can be expected that the preference for O−H bond activation over that of the Ln−O bond should be feasible. Recently, we began a research program to explore the modification method of the ligands of organolanthanide complexes.[5] In a previous work, we observed an unexpected interaction of the adjacent NH_2 group with the isocyanate unit inserted into the lanthanide−sulfur bond, allowing for the construction of a coordinated thiazole ring.[12] To probe the extent of ligand-based reactions and to develop some new methods for the construction of support ligands in organolanthanide chemistry, we are especially interested in finding out whether the selective O−H transformation was accessible on organolanthanide hydroxide complexes. We describe herein the reactions of lanthanocene hydroxides with ketene, isocyanate, lanthanocene alkyl, and triscyclopentadienyl lanthanide complexes, which lead to the isolation and characterization of a series of lanthanocene carboxylate, carbaminate, and μ-oxo derivatives, and demonstrate the potential of organolanthanide hydroxides as precursors in the synthesis of organolanthanide complexes.

Experimental Section

General Procedure. All operations involving air- and moisture-sensitive compounds were carried out under purified nitrogen with rigorous exclusion of air and water by standard Schlenk and glovebox techniques. All solvents were refluxed and distilled over sodium benzophenone ketyl under nitrogen immediately prior to use. Cp_3Ln,[13] $[Cp_2Ln(\mu\text{-}OH)(THF)]_2$,[14] $Cp_2Ln^nBu(THF)_x$,[15] $[Cp_2Ln(\mu\text{-}CH_3)]_2$,[16] and ethylphenyl ketene[17] were prepared according to the procedures described in the literature. Li^{n}Bu, $LiCH_3$, and PhNCO were purchased from Aldrich and used without purification. Elemental analyses for C, H, and N were carried out on a VARIO EL III CHN-O analyzer. Metal analyses for lanthanides were carried out by complexometric titration with EDTA. Infrared spectra were obtained on a NICOLET FT-IR 360 spectrometer with samples prepared as Nujol mulls. Mass spectra were recorded on a Philips Agilent MS5973N instrument operating in the EI mode. Crystalline samples of the respective complexes were rapidly introduced by the direct inlet techniques with a source temperature of 200 °C. The values of *m*/*z* refer to the isotopes ^{1}H,^{12}C, ^{14}N, ^{89}Y, ^{166}Er, and ^{174}Yb. ^{1}H NMR data were obtained on a Bruker DMX-500 NMR spectrometer and were referenced to residual protons in THF-d_8 (1.72, 3.58) C_6D_6 (δ 7.16). Melting points were determined in a sealed, nitrogen-filled capillary and were uncorrected.

Synthesis of $[Cp_2Y(\mu\text{-}OH)(THF)]_2$ (1). The cooled, degassed H_2O (27 mg, 1.48 mmol) in THF (35 mL) was slowly (about 5 min) added to a solution of Cp_3Y (421 mg, 1.48 mmol) in THF (50 mL) at −80 °C. The reaction mixture was slowly warmed to room temperature and stirred overnight. The solution was then concentrated to ca. 50 mL and cooled at −18 °C to give **1** as colorless crystals. Yield: 223 mg, 49%. IR (Nujol, cm^{-1}): 3556 m, 3063 m, 1639 s, 1486 m, 1346 m, 1249 m, 1173 m, 1060 m, 1012 s, 926 s, 766 s. ^{1}H NMR (THF-d_8): 6.10 (s, 10H, C_5H_5), 3.60 (t, 4H, THF), 1.77 (m, 4H, THF). Anal. Calcd for $C_{28}H_{38}O_4Y_2$: C, 54.56; H, 6.21. Found: C, 54.91; H, 6.06.

Synthesis of $[Cp_2Er(\mu\text{-}OH)(THF)]_2$ (2). Following the above procedure described for **1**, reaction of H_2O (25 mg, 1.37 mmol) with Cp_3Er (497 mg, 1.37 mmol) gave **2** as pink crystals. Yield: 275 mg, 52%. IR (Nujol, cm^{-1}): 3550 m, 3088 m, 1636 s, 1438 s, 1173 m, 1071 s, 1007 s, 914 s, 768 s. Anal. Calcd for $C_{28}H_{38}O_4Er_2$: C, 43.51; H, 4.95. Found: C, 42.98; H, 5.02.

Synthesis of $[Cp_2Yb(\mu\text{-}OH)(THF)]_2$ (3) and $[Cp_2Yb]_2(\mu\text{-}OH)_2(\mu_3\text{-}O)[(YbCp)(THF)]$ (4). To a 55 mL THF solution of Cp_3Yb (642 mg, 1.74 mmol) was added cooled, degassed H_2O (31 mg, 1.74 mmol) in THF (30 mL) at −80 °C. The mixture changed from dark green to orange-yellow immediately. After being stirred for 10 min, the solution was concentrated to ca. 45 mL to give a yellow solid, which was isolated by filtration followed by subsequent washing with a minimal amount of a mixture of THF and *n*-hexane.

(6) (a) Christianson, D. W.; Fierke, C. A. *Acc. Chem. Res.* **1996**, *29*, 331−339. (b) Jabri, E.; Carr, M. B.; Hausinger, R. P.; Karplus, P. A. *Science* **1995**, *268*, 998−1004. (c) Lipscomb, W. N.; Sträter, N. *Chem. Rev.* **1996**, *96*, 2375−2433 and references therein. (d) Christianson, D. W.; Cox, J. D. *Annu. Rev. Biochem.* **1999**, *68*, 33−57. (e) Fulton, J. R.; Holland, A. W.; Fox, D. J.; Bergman, R. G. *Acc. Chem. Res.* **2002**, *35*, 44−56. (f) Jayaprakash, K. N.; Conner, D.; Gunnoe, T. B. *Organometallics* **2001**, *20*, 5254−5256. (g) Conner, D.; Jayaprakash, K. N.; Gunnoe, T. B.; Boyle, P. D. *Inorg. Chem.* **2002**, *41*, 3042−3049. (h) Bergquist, C.; Fillebeen, T.; Morlok, M. M.; Parkin, G. *J. Am. Chem. Soc.* **2003**, *125*, 6189−6199. (i) Cuesta, L.; Hevia, E.; Morales, D.; Pérez, J.; Riera, L.; Miguel, D. *Organometallics* **2006**, *25*, 1717−1722.

(7) (a) Scarrow, R. C.; Brennan, B. A.; Cummings, J. G.; Jin, H.; Duong, D. J.; Kindt, J. T.; Nelson, M. J. *Biochemistry* **1996**, *35*, 10078−10088. (b) Brennan, B. A.; Alms, G.; Nelson, M. J.; Durney, L. T.; Scarrow, R. C. *J. Am. Chem. Soc.* **1996**, *118*, 9194−9195.

(8) (a) Nelson, M. J. *J. Am. Chem. Soc.* **1988**, *110*, 2985−2986. (b) Scarrow, R. C.; Trimitsis, M. G.; Buck, C. P.; Grove, G. N.; Cowling, R. A.; Nelson, M. J. *Biochemistry* **1994**, *33*, 15219−15229.

(9) (a) Wilcox, D. E. *Chem. Rev.* **1996**, *96*, 2435−2458. (b) Klabunde, T.; Sträter, N.; Fröhlich, R.; Witzel, H.; Krebs, B. *J. Mol. Biol.* **1996**, *259*, 737−748.

(10) Hoganson, C. W.; Babcock, G. T. *Science* **1997**, *277*, 1953−1956.

(11) Schumann, H.; Meese-Marktscheffel, J. A.; Esser, L. *Chem. Rev.* **1995**, *95*, 865−986.

(12) Zhang, J.; Ma, L. P.; Cai, R. F.; Weng, L. H.; Zhou, X. G. *Organometallics* **2005**, *24*, 738−742.

(13) Birmingham, J. M.; Wilkinson, G. *J. Am. Chem. Soc.* **1956**, *78*, 42−44.

(14) (a) Evans, W. J.; Hozbor, M. A.; Bott, S. G.; Robinson, G. H.; Atwood, J. L. *Inorg. Chem.* **1988**, *27*, 1990−1993. (b) Schumann, H.; Loebel, J.; Pickardt, J. *Organometallics* **1991**, *10*, 215−219. (c) Hitchcock, P. B.; Lappert, M. F.; Prashar, S. *J. Organomet. Chem.* **1991**, *413*, 79−90. (d) Deng, D. L.; Song, F. Q.; Wang, Z. Y.; Qian, C. T. *Polyhedron* **1992**, *11*, 2883−2887.

(15) (a) Schumann, H.; Genthe, W.; Bruncks, N. *Angew. Chem., Int. Ed.* **1981**, *20*, 119−120. (b) Zhou, X. G.; Zhang, L. B.; Zhu, M.; Cai, R. F.; Weng, L. H.; Huang, Z. X.; Wu, Q. *J. Organometallics* **2001**, *20*, 5700−5706.

(16) (a) Ely, N. M.; Tsutsui, M. *Inorg. Chem.* **1975**, *14*, 2680−2687. (b) Evans, W. J.; Dominguez, R.; Hanusa, T. P. *Organometallics* **1986**, *5*, 263−270.

(17) Baigrie, L. M.; Seiklay, H. R.; Tidwell, T. T. *J. Am. Chem. Soc.* **1985**, *107*, 5391−5396.

Yield: 218 mg, 32%. Anal. Calcd for $C_{28}H_{38}O_4Yb_2$: Yb, 44.12. Found: 44.82.

The above mother liquid was kept for 2 days at room temperature and was then concentrated to ca. 3 mL. Yellow crystals of **4**·2THF were obtained at −18 °C. Yield: 219 mg, 34%. IR (Nujol, cm^{-1}): 3447 m, 3088 m, 1619 m, 1291 w, 1260 w, 1187 w, 1055 s, 1010 s, 875 s, 750 s. Anal. Calcd for $C_{37}H_{51}O_6Yb_3$: C, 40.00; H, 4.63. Found: C, 40.19; H, 4.55.

Synthesis of [$Cp_2Yb(\mu$-η^1:η^2-$O_2CCHEtPh)]_2$ (5). To a solution of **3** (467 mg, 0.60 mmol) in 30 mL of THF was added PhEtCCO (174 mg, 1.19 mmol) at −50 °C. After being stirred for 30 min at low temperature, the mixture was slowly warmed to room temperature and stirred overnight. The color of the solution changed from yellow to orange-red slowly. The solution was then concentrated and cooled at −18 °C to give **5** as orange-yellow crystals. Yield: 477 mg, 86%. Mp: 234−236 °C. IR (Nujol, cm^{-1}): 1671 m, 1571 s, 1413 s, 1335 s, 1291 s, 1240 s, 1291 s, 1239 s, 1184 m, 1076 m, 1011 s, 907 m, 786 s, 703 m, 582 s. EI-MS *m*/*z* (fragment, relative intensity (%)): 467 (M/2, 30), 402 (M/2−Cp, 15), 304 (Cp_2Yb, 5), 219 (M/2−2Cp−PhEtCH + 1, 85), 66 (CpH, 60). Anal. Calcd for $C_{40}H_{42}O_4Yb_2$: C, 51.50; H, 4.54. Found: C, 51.68; H, 4.39.

Synthesis of [$Cp_2Er(\mu$-η^1:η^2-$O_2CCHEtPh)]_2$ (6). To a 30 mL of solution of **2** (382 mg, 0.50 mmol) in THF was added PhEtCCO (145 mg, 0.989 mmol) at −50 °C. The mixture was allowed to slowly warm to room temperature and stirred overnight. The solvent was then evaporated by reduced pressure to ca. 8 mL. Recrystallization by vapor diffusion of hexane into the THF solution afforded pink crystals. Yield: 383 mg, 84%. Mp: 279−280 °C. IR (Nujol, cm^{-1}): 1668 m, 1569 s, 1409 s, 1335 m, 1294 m, 1239 s, 1184 m, 1075 m, 1009 s, 907 s, 781 s, 700 m, 582 s. EI-MS *m*/*z* (fragment, relative intensity(%)): 459 (M/2, 5), 394 (M/2−Cp, 10), 296 (Cp_2-Er, 100), 146 (PhEtCCO, 2), 66 (CpH, 80). Anal. Calcd for $C_{40}H_{42}O_4Er_2$: C, 52.15; H, 4.59. Found: C, 52.09; H, 4.70.

Synthesis of [$Cp_2Y(\mu$-η^1:η^2-$O_2CCHEtPh)]_2$ (7). Following the above procedure described for **5**, reaction of **1** (327 mg, 0.53 mmol) with PhEtCCO (155 mg, 1.06 mmol) gave **7** as yellow crystals. Yield: 315 mg, 78%. Mp: 271−272 °C. ^{1}H NMR (C_6D_6): δ 6.60 (s, 5H, C_5H_5), 6.40 (s, 5H, C_5H_5), 2.46 (t, 1H, $CHCH_2$), 1.24 (m, 2H, CH_2CH_3), 0.89 (t, 3H, CH_2CH_3). IR (Nujol, cm^{-1}): 1668 m, 1570 s, 1409 m, 1336 m, 1287 m, 1239 s, 1184 m, 1075 s, 1009 s, 907 s, 781 s, 700 m, 580 s. EI-MS *m*/*z* (fragment, relative intensity (%)): 699 (M−Cp, 100), 382 (M/2, 5), 317 (M/2−Cp, 8), 219 (Cp_2Y, 30), 65 (Cp, 5). Anal. Calcd for $C_{40}H_{42}O_4Y_2$: C, 62.84; H, 5.54. Found: C, 62.77; H, 5.58.

Synthesis of [$Cp_2Y(THF)]_2(\mu$-η^2:η^2-$O_2CNPh)$ (8). Method A. To a solution of **1** (468 mg, 0.76 mmol) in THF (30 mL) was added PhNCO (181 mg, 1.52 mmol) at −50 °C. After being stirred for 30 min at low temperature, the mixture was slowly warmed to room temperature and stirred overnight. The solution was then concentrated, and some days later, yellow crystals of **8** were obtained at room temperature. Yield: 141 mg, 26%. ^{1}H NMR (C_6D_6): δ 7.16 (m, 5H, Ph), 6.49 (s, 10H, C_5H_5), 6.30 (s, 10H, C_5H_5), 3.57 (t, 8H, THF), 1.42 (m, 8H, THF). IR (Nujol, cm^{-1}): 1607 s, 1585 s, 1502 s, 1260 m, 1236 m, 1199 w, 1178 w, 1052 m, 1014 m, 888 w, 773 s, 691 s, 662 s, 640 m. EI-MS *m*/*z* (fragment, relative intensity (%)): 645 (M−2THF, 5), 626 (M−PhN, 5), 349 (M−Cp_2Y−Ph−THF, 20), 219 (Cp_2Y, 50), 66 (CpH, 50). Anal. Calcd for $C_{35}H_{41}O_4NY_2$: C, 58.59; H, 5.76; N, 1.95. Found: C, 58.70; H, 5.82; N, 1.86.

Method B. To a solution of **1** (191 mg, 0.31 mmol) in THF (35 mL) was added PhNCO (73 mg, 0.62 mmol) at −50 °C. Five minutes later, a solution of Cp_3Y (175 mg, 0.62 mmol) in THF (25 mL) was added to the mixture. The reaction mixture was slowly warmed to room temperature and stirred overnight. The solution was evaporated to ca. 10 mL to give **8** as pale yellow crystals. Yield: 351 mg, 79%.

Synthesis of [$Cp_2Yb(THF))_2(\mu$-η^2:η^2-$O_2CNPh)$ (9). To a solution of **3** (224 mg, 0.29 mmol) in THF (20 mL) was added PhNCO (67 mg, 0.57 mmol) at −50 °C. Five minutes later, a solution of Cp_3Yb (209 mg, 0.57 mmol) in THF (20 mL) was added to the mixture. After being stirred for 30 min at low temperature, the reaction mixture was slowly warmed to room temperature and stirred overnight; the color of the solution changed from green to orange gradually. The solvent was evaporated by reduced pressure to ca. 8 mL, and orange crystals of **9** were obtained by vapor diffusion of hexane into THF solution. Yield: 452 mg, 89%. IR (Nujol, cm^{-1}): 1605 s, 1584 m, 1533 s, 1266 m, 1247 m, 1178 w, 1065 m, 1013 s, 885 m, 769 s, 694 s, 667 s. Anal. Calcd for $C_{35}H_{41}O_4NYb_2$: C, 47.46; H, 4.67; N, 1.58. Found: C, 47.38; H, 4.69; N, 1.49.

Synthesis of [$Cp_2Er(THF)]_2(\mu$-η^2:η^2-$O_2CNPh)$ (10). Following the procedure described above for **9**, reaction of **2** (245 mg, 0.32 mmol) with PhNCO (76 mg, 0.635 mmol) immediately followed by treatment of Cp_3Er (230 mg, 0.635 mmol) in THF gave **10** as pink crystals. Yield: 461 mg, 83%. IR (Nujol, cm^{-1}): 1607 s, 1580 s, 1502 s, 1260 m, 1236 m, 1177 w, 1052 m, 1013 s, 891 w, 764 s, 692 s. Anal. Calcd for $C_{35}H_{41}O_4NEr_2$: C, 48.09; H, 4.73; N, 1.60. Found: C, 48.11; H, 4.62; N, 1.73.

Synthesis of [$Cp_2Yb(THF)]_2(\mu$-O) (11). Method A. To a 25 mL THF solution of **3** (298 mg, 0.38 mmol) was added the solution of Cp_3Yb (281 mg, 0.76 mmol) in THF (20 mL) at −50 °C. The green mixture was stirred for 3 days. The solvent was then evaporated to ca. 7 mL. Some days later, yellow green crystals of **11** were obtained at room temperature. Yield: 444 mg, 76%. IR (Nujol, cm^{-1}): 3089 m, 1438 s, 1058 m, 1010 s, 917 m, 781 s. Anal. Calcd for $C_{28}H_{36}O_3Yb_2$: C, 43.87; H, 4.73. Found: C, 43.92; H, 4.66.

Method B. To a 30 mL THF solution of **3** (396 mg, 0.50 mmol) was added a solution of $[Cp_2Yb(\mu$-$CH_3)]_2$ (311 mg, 0.50 mmol) in 30 mL of toluene at −50 °C. The color of the mixture changed from yellow to green quickly. After being stirred overnight, the solution was concentrated, and yellow green crystals of **11** were obtained at room temperature. Yield: 351 mg, 72%.

Synthesis of ($Cp_2Er)_3(\mu$-OH)(μ_3-O)(μ-Cl)Li$(THF)_4$ (12). To a solution of Cp_2ErCl (589 mg, 1.77 mmol) in THF (30 mL) was added *n*-butyllithium (1.604 M, in cyclohexane, 1.10 mL) at −30 °C. After being stirred for 4 h, a THF solution of **2** (684 mg, 0.89 mmol) at −20 °C was added to the mixture. The reaction mixture was then warmed to ambient temperature and stirred overnight. The solution was concentrated and cooled at −18 °C to give **12** as pink crystals. Yield: 556 mg, 37.5% (on the basis of Er). Mp: 227−229 °C. IR (Nujol, cm^{-1}): 3504 m, 3089 m, 2717 m, 1743 w, 1621 m, 1460 s, 1294 m, 1246 m, 1173 m, 1042 s, 1009 s, 914 s, 890 s, 773 s, 664 s. EI-MS *m*/*z* (fragment, relative intensity (%)): 296 (Cp_2Er, 100), 66 (CpH, 35). Anal. Calcd for $C_{46}H_{63}O_6Er_3LiCl$: C, 43.98; H, 5.02. Found: C, 44.01; H, 5.11.

X-ray Data Collection, Structure Determination, and Refinement of 1, 2, and 4−12. Suitable crystals of complexes **1**, **2** and **4−12** were selected and sealed under argon in Lindemann glass capillaries for X-ray structural analysis. Diffraction data were collected on a Bruker SMART CCD diffractometer using graphite-monochromated Mo K_α (λ = 0.71073 Å) radiation. During the collection of the intensity data, no significant decay was observed. For **1**, frames were integrated to a maximum 2θ angle of 52.00° with the Siemens SAINT program to yield a total of 6168 reflections, of which 2656 were independent (R_{int} = 0.0476). For

Table 1. Crystal and Data Collection Parameters of Complexes **1**, **2**, and **4**·2THF

	1	**2**	**4**·2THF
formula	$C_{28}H_{38}O_4Y_2$	$C_{28}H_{38}Er_2O_4$	$C_{37}H_{51}O_6Yb_3$
mol wt	616.40	773.09	1110.9
cryst color	colorless	pink	orange-yellow
cryst dimensions (mm^3)	0.20× 0.15 × 0.15	0.20× 0.20 × 0.10	0.35× 0.25 × 0.20
cryst syst	monoclinic	monoclinic	orthorhombic
space group	*P*2(1)/*c*	*P*2(1)/*c*	*Pbcm*
a (Å)	7.606(2)	7.593(3)	11.5420(15)
b (Å)	20.370(6)	20.271(8)	14.977(2)
c (Å)	9.034(3)	8.999(3)	22.309(3)
α (deg)	90	90	90
β (deg)	105.085(4)	104.861(5)	90
γ (deg)	90	90	90
V ($Å^3$)	1351.4(7)	1338.8(9)	3856.5(9)
Z	2	2	4
D_{calcd} (g cm^{-3})	1.515	1.918	1.913
μ (mm^{-1})	4.303	6.256	7.256
F(000)	632	748	2124
radiation (*λ* = 0.710730Å)	Mo Kα	Mo Kα	Mo Kα
T (K)	293(2)	293(2)	293(2)
scan type	*ω*−2*θ*	*ω*−2*θ*	*ω*−2*θ*
θ range (deg)	2.00−26.00	2.55−26.01	2.23−26.01
no. of reflns measured	6168	5989	21347
no. of unique reflns	2656 (R_{int} = 0.0476)	2618 (R_{int} = 0.0635)	3898 (R_{int} = 0.0506)
completeness to *θ (%)*	99.9 (*θ* = 26.00°)	99.4 (*θ* = 26.01°)	99.9 (*θ* = 26.01°)
max. and min. transmission	0.5646 and 0.4799	0.5735 and 0.3676	0.3248 and 0.1856
data/restraints/params	2656/1/158	2618/0/158	3898/1/218
GOF on F^2	0.891	1.108	1.108
R1,[a] wR2[b] ($I > 2\sigma(I)$)	0.0351, 0.0743	0.0407, 0.0975	0.0372, 0.0791
R1,[a] wR2[b] (all data)	0.0585, 0.0781	0.0526, 0.1022	0.0660, 0.1018
largest diff. peak and hole (e $Å^{-3}$)	0.413 and −0.361	0.941 and −1.491	1.401 and −1.063

[a] $R1 = \sum||F_o| - |F_c||/\sum|F_o|$. [b] $wR2 = [\sum w(F_o^2 - F_c^2)^2/\sum w(F_o^2)^2]^{1/2}$.

2, frames were integrated to a maximum 2*θ* angle of 52.02° with the Siemens SAINT program to yield a total of 5989 reflections, of which 2618 were independent (R_{int} = 0.0635). For **4**·2THF, frames were integrated to a maximum 2*θ* angle of 52.02° with the Siemens SAINT program to yield a total of 21 347 reflections, of which 3898 were independent (R_{int} = 0.0506). For **5**, frames were integrated to a maximum 2*θ* angle of 50.00° with the Siemens SAINT program to yield a total of 4661 reflections, of which 2970 were independent (R_{int} = 0.0264). For **6**, frames were integrated to a maximum 2*θ* angle of 52.02° with the Siemens SAINT program to yield a total of 7968 reflections, of which 3520 were independent (R_{int} = 0.0322). For **7**, frames were integrated to a maximum 2*θ* angle of 50.02° with the Siemens SAINT program to yield a total of 7341 reflections, of which 3205 were independent (R_{int} = 0.0728). For **8**, frames were integrated to a maximum 2*θ* angle of 50.02° with the Siemens SAINT program to yield a total of 13 556 reflections, of which 5764 were independent (R_{int} = 0.0949). For **9**, frames were integrated to a maximum 2*θ* angle of 50.02° with the Siemens SAINT program to yield a total of 13 116 reflections, of which 5667 were independent (R_{int} = 0.0705). For **10**, frames were integrated to a maximum 2*θ* angle of 50.02° with the Siemens SAINT program to yield a total of 13 399 reflections, of which 5720 were independent (R_{int} = 0.0274). For **11**, frames were integrated to a maximum 2*θ* angle of 50.02° with the Siemens SAINT program to yield a total of 5583 reflections, of which 2394 were independent (R_{int} = 0.0261). For **12**, frames were integrated to a maximum 2*θ* angle of 52.02° with the Siemens SAINT program to yield a total of 20 109 reflections, of which 8354 were independent (R_{int} = 0.0461). The final unit-cell parameters were determined from the full-matrix least-squares on F^2 refinement of three-dimensional centroids of 2656 reflections for **1**, 2618 reflections for **2**, 3898 reflections for **4**·2THF, 2970 reflections for **5**, 3520 reflections for **6**, 3205 reflections for **7**, 5764 reflections for **8**, 5667 reflections for **9**, 5720 reflections for **10**, 2394 reflections for **11**, and 8354 reflections for **12**.

The intensities were corrected for Lorentz-polarization effects and empirical absorption with the SADABS program.[18] The structures were solved by the direct method using the SHELXLS-97 program[19] and refined with all data by full-matrix least-squares on F^2. The H atoms were included in calculated positions with isotropic thermal parameters related to those of the supporting carbon atoms, but were not included in the refinement. A summary of the crystallographic data is given in Tables 1−3.

Results and Discussion

Synthesis of [Cp$_2$Ln(*μ*-OH)(THF)]$_2$ and [Cp$_2$Yb(*μ*-OH)]$_2$[CpYb(THF)](*μ*$_3$-O). Starting materials [$Cp_2Ln(\mu$-OH)(THF)]$_2$ (Ln = Y (**1**), Er (**2**), Yb (**3**)) were prepared in mediate yields by reaction of H_2O with the corresponding Cp_3Ln in THF at low temperature. The elimination of CpH and the formation of the hydroxide complexes were confirmed by GC-MS, IR, elemental analyses, and X-ray structural analyses. Noticeably, [$Cp_2Yb(\mu$-OH)(THF)]$_2$ (**3**) is unstable and can be converted to [$Cp_2Yb(\mu$-OH)]$_2$[CpYb(THF)](μ_3-O) (**4**) when treated with THF at room temperature for a long time. **4** is stable and does not react further under the given conditions. Therefore, to obtain the best results, **3** should be prepared immediately prior to use. However, elimination of CpH for **1** and **2** was not observed, even in warm THF. This difference is in agreement with the

(18) Sheldrick, G. M. *SADABS, A Program for Empirical Absorption Correction*; University of Göttingen: Göttingen, Germany, 1998.
(19) Sheldrick, G. M. *SHELXL-97, Program for Refinement of the Crystal Structure*; University of Göttingen: Göttingen, Germany, 1997.

Table 2. Crystal and Data Collection Parameters of Complexes **5**−**8**

	5	**6**	**7**	**8**
formula	$C_{40}H_{42}O_4Yb_2$	$C_{40}H_{42}Er_2O_4$	$C_{40}H_{42}Y_2O_4$	$C_{35}H_{41}NO_4Y_2$
mol wt	932.82	921.26	764.56	717.51
cryst dimensions (mm^3)	0.05× 0.05 × 0.10	0.20× 0.15 × 0.15	0.25× 0.15 × 0.10	0.20× 0.10 × 0.10
cryst syst	monoclinic	monoclinic	monoclinic	monoclinic
space group	*P*2(1)/*c*	*P*2(1)/*c*	*P*2(1)/*c*	*P*2(1)/*c*
a (Å)	10.770(4)	10.787(4)	10.811(8)	17.141(5)
b (Å)	8.474(3)	8.545(3)	8.599(7)	16.160(4)
c (Å)	19.313(7)	19.523(7)	19.625(9)	11.854(3)
α (deg)	90	90	90	90
β (deg)	90.797(5)	90.759(5)	90.586(12)	94.331(5)
γ (deg)	90	90	90	90
V ($Å^3$)	1762.3(11)	1799.4(11)	1824(2)	3274.3(15)
Z	2	2	2	4
D_{calcd} (g cm^{-3})	1.758	1.700	1.392	1.456
μ (mm^{-1})	5.313	4.670	3.203	3.564
F(000)	908	900	784	1472
T (K)	298(2)	293(2)	293(2)	293(2)
θ range (deg)	1.89−25.00	1.89−26.01	1.88−25.01	1.19−25.01
no. of reflns measured	4661	7968	7341	13 556
no. of unique reflns	2970 (R_{int} = 0.0264)	3520 (R_{int} = 0.0322)	3205 (R_{int} = 0.0728)	5764 (R_{int} = 0.0949)
completeness to *θ* (%)	95.9 (*θ* = 25.00°)	99.5 (*θ* = 26.01°)	99.3 (*θ* = 25.01°)	100 (*θ* = 25.01°)
max. and min. transmission		0.5409 and 0.4552	0.7401 and 0.5015	0.7170 and 0.5358
data/restraints/params	2970/36/209	3520/0/208	3205/0/208	5764/0/379
GOF on F^2	1.062	1.072	0.986	0.651
R1,[a] wR2[b] ($I > 2\sigma(I)$)	0.0371, 0.0867	0.0312, 0.0609	0.0619, 0.1414	0.0472, 0.0485
R1,[a] wR2[b] (all data)	0.0502, 0.0938	0.0427, 0.0643	0.1031, 0.1619	0.1487, 0.0598
largest diff. peak and hole (e•$Å^{-3}$)	1.118 and −0.943	0.910 and −0.416	1.124 and −0.815	0.515 and −0.406

[a] $R1 = \sum||F_o| - |F_c||/\sum|F_o|$. [b] $wR2 = [\sum w(F_o^2 - F_c^2)^2/\sum w(F_o^2)^2]^{1/2}$.

Table 3. Crystal and Data Collection Parameters of Complexes **9**−**12**

	9	**10**	**11**	**12**
formula	$C_{35}H_{41}NO_4Yb_2$	$C_{35}H_{41}NO_4Er_2$	$C_{28}H_{36}O_3Yb_2$	$C_{46}H_{63}ClEr_3LiO_6$
mol wt	885.77	874.21	766.65	1256.12
cryst dimensions (mm^3)	0.25× 0.20 × 0.20	0.25× 0.25 × 0.20	0.10× 0.15 × 0.20	0.20× 0.15 × 0.10
cryst syst	monoclinic	monoclinic	monoclinic	orthorhombic
space group	*P*2(1)/*c*	*P*2(1)/*c*	*C*2/*c*	*P*2(1)2(1)2(1)
a (Å)	17.103(11)	17.132(5)	13.138(4)	10.962(3)
b (Å)	16.043(10)	16.122(5)	10.039(3)	15.106(4)
c (Å)	11.792(7)	11.839(4)	21.099(7)	28.887(7)
α (deg)	90	90	90	90
β (deg)	94.370(8)	94.353(4)	102.521(4)	90
γ (deg)	90	90	90	90
V ($Å^3$)	3226(3)	3260.6(17)	2716.6(15)	4784(2)
Z	4	4	4	4
D_{calcd} (g cm^{-3})	1.824	1.781	1.875	1.741
μ (mm^{-1})	5.8	5.150	6.868	5.313
F(000)	1720	1704	1472	2436
T (K)	293(2)	293(2)	293(2)	298(2)
θ range (deg)	1.74−25.01	1.74−25.01	1.98−25.01	1.41−25.01
no. of reflns measured	13 116	13 399	5583	20 109
no. of unique reflns	5667 (R_{int} = 0.0705)	5720 (R_{int} = 0.0274)	2394 (R_{int} = 0.0261)	8354 (R_{int} = 0.0461)
completeness to *θ* (%)	99.9 (*θ* = 25.01°)	99.7 (*θ* = 25.01°)	100 (*θ* = 25.01°)	99.9 (*θ* = 25.01°)
max. and min. transmission	0.3900 and 0.3250	0.4257 and 0.3592		0.6186 and 0.4163
data/restraints/params	5667/0/354	5720/0/380	2394/0/152	8354/7/494 1.072
GOF on F^2	0.967	0.989	1.204	1.037
R1,[a] wR2[b] ($I > 2\sigma(I)$)	0.0506, 0.1199	0.0261, 0.0548	0.0347, 0.0796	0.0474, 0.0916
R1,[a] wR2[b] (all data)	0.0718, 0.1309	0.0389, 0.0585	0.0425, 0.0819	0.0659, 0.0986
largest diff. peak and hole (e•$Å^{-3}$)	2.186 and −2.953	0.986 and −0.660	1.050 and −0.842	0.883 and −0.512

[a] $R1 = \sum||F_o| - |F_c||/\sum|F_o|$. [b] $wR2 = [\sum w(F_o^2 - F_c^2)^2/\sum w(F_o^2)^2]^{1/2}$.

observation in the reaction of $HC[CMeN(C_6H_3{}^iPr_2\text{-}2,6)]_2$-AlMe(OH) with Cp_3Ln, in which acid displacement of cyclopentadienyl ligands from a heavy rare earth moiety is also easier than that from mediate ones.[20] In addition, water should be added within a short time in the preparation of **1**−**3**, because they can react slowly with Cp_3Ln precursors (see below). These results indicate that the number of cyclopentadienyl groups liberated from a Cp_3Ln moiety is largely influenced by the size of the lanthanide ions.

Reaction of $[Cp_2Ln(\mu\text{-}OH)(THF)]_2$ with PhEtCCO. As illustrated in Scheme 1, $[Cp_2Ln(\mu\text{-}OH)(THF)]_2$ reacted with 2 equiv of PhEtCCO in THF to give the products from formal PhEtCCO insertion into the O−H bond, $[Cp_2Ln(\mu\text{-}\eta^1{:}\eta^2\text{-}O_2CCHEtPh)]_2$ (Ln = Yb (**5**), Er (**6**), Y (**7**)), as determined by X-ray crystal analysis. Studies on the reactivity of organo-

(20) Chai, J. F.; Jancik, V.; Singh, S.; Zhu, H. P.; He, C.; Roesky, H. W.; Schmidt, H.-G.; Noltemeyer, M.; Hosmane, N. S. *J. Am. Chem. Soc.* **2005**, *127*, 7521−7528.

Scheme 1

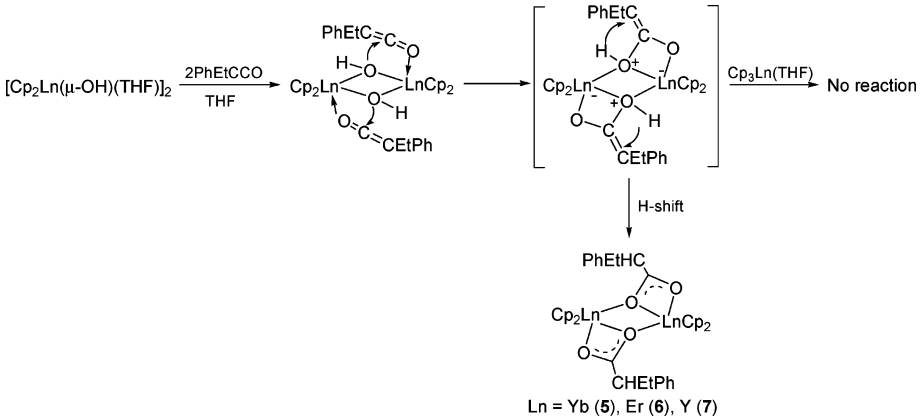

metallic hydroxide complexes are scarce, and there are fewer examples involving the bridging hydroxide ligands because of the lower nucleophilicity compared with the terminal ligands. To the best of our knowledge, no example of reactions of organometallic complexes containing bridging OH groups with unsaturated organic electrophiles, which proceed smoothly with terminal hydroxide complexes, has been reported. During the revision of this manuscript, Pérez and co-workers reported the first reaction of ketenes with transition-metal hydroxide complexes, but the hydroxide groups also act as the terminal ligands.[6i]

The insertion of unsaturated substrates into the organolanthanide complexes is regarded as one of the most fundamental organometallic reactions and is attracting great interest as a basis for the lanthanide-promoted functionalization and polymerization reactions.[21] Despite significant advances in insertion reactions of functionalized organic molecules into the Ln−H, Ln−C, Ln−N, Ln−P, and Ln−S bonds, the corresponding insertions into the lanthanide−oxygen or heteroatom−hydrogen bond of organolanthanides have remained almost unexplored to date.[21] On the other hand, the synthesis of lanthanide carboxylate complexes has become increasingly important because of their potential applications in catalysts and new materials.[22] Despite the availability of various procedures for the preparation of lanthanide carboxylate complexes, the carboxylate ligands are generally synthesized prior to complexes[10] or constructed by the insertion of CO_2 into the lanthanide-ligand bond.[23] Therefore, the formation of **5**−**7** not only represents the first example of the formal addition of unsaturated molecules to the O−H bond of organolanthanide hydroxides but also provides a new route to lanthanide carboxylate complexes.

Reaction of $[Cp_2Ln(\mu\text{-}OH)(THF)]_2$ with PhNCO. Although the selective transformations of the OH ligand are fairly common in transition-metal chemistry,[6−10] no example of the regioselective O−H addition of organolanthanide hydroxides has been reported previously. The above observation prompted us to further explore the reactivity of lanthanocene hydroxides with phenyl isocyanate. In contrast to the reaction with ketene, treatment of $[Cp_2Y(\mu\text{-}OH)(THF)]_2$ with 2 equiv of PhNCO led to the isolation of unexpected product $[Cp_2Y(THF)]_2(\mu\text{-}\eta^2\text{:}\eta^2\text{-}O_2CNPh)$ (**8**) in 26% yield, with elimination of CpH identified by GC/MS. The formation of compound **8** can be attributed to the intramolecular CpH elimination of the cycloaddition intermediate (**I**) to $[CpY(OCONPh)(THF)]_2$ (**III**) followed by rearrangement, as indicated in Scheme 2. To the best of our knowledge, this type of reaction is unique; previously, reactions of other metal-hydroxide complexes generally gave the products from formal O−H or M−OH addition to the C═N bond of isocyanates.[24] However, attempts to isolate another rearrangement product, $Y_2(O_2CNPh)_3$, and one or more of the intermediates **I**−**III** in Scheme 2 were unsuccessful. The driving force for the CpH elimination reaction of the putative amido intermediates probably results from the acidity of the N−H (or conjugate oxonium form **I**) proton and the basicity of the cyclopentadienyl ligand. Consistent with this notion, treatment of $[Cp_2Ln(\mu\text{-}OH)(THF)]_2$ with 2 equiv of PhNCO followed by reaction with stoichiometric Cp_3Ln afforded $[Cp_2Ln(THF)]_2(\mu\text{-}\eta^2\text{:}\eta^2\text{-}O_2CNPh)$ (Ln = Y(**8**), Yb(**9**), Er(**10**)) in excellent yield with complete chemoselectivity. However, by contrast with PhNCO, attempts to trap the hydrogen atom of the oxonium intermediate using Cp_3Ln as a H-acceptor are unsuccessful in the reaction procedure of $[Cp_2Ln(\mu\text{-}OH)(THF)]_2$ with PhEtCCO, in which the more-

(21) (a) Evans, W. J.; Davis, B. L. *Chem. Rev.* **2002**, *102*, 2119−2136. (b) Ferrence, G. M.; Takats, J. *J. Organomet. Chem.* **2002**, *647*, 84−93. (c) Zhou, X. G.; Zhu, M. *J. Organomet. Chem.* **2002**, *647*, 28−49.

(22) (a) Evans, W. J.; Giarikos, D. G.; Ziller, J. W. *Organometallics* **2001**, *20*, 5751−5758. (b) Evans, W. J.; Giarikos, D. G. *Macromolecules* **2004**, *37*, 5130−5132. (c) Stone, D. L.; Dykes, G. M.; Smith, D. K. *Dalton Trans.* **2003**, 3902−3906. (d) Lam, A. W. H.; Wong, W. T.; Gao, S.; Wen, G. H.; Zhang, X. X. *Eur. J. Inorg. Chem.* **2003**, 149−163. (e) Ghosh, S. K.; Bharadwaj, P. K. *Eur. J. Inorg. Chem.* **2005**, 4886−4889. (f) Song, J. L.; Lei, C.; Mao, J. G. *Inorg. Chem.* **2004**, *43*, 5630−5634. (g) Arnaud, N.; Georges, J. *Analyst* **2000**, *125*, 1487−1490.

(23) (a) Evans, W. J.; Perotti, J. M.; Ziller, J. W. *J. Am. Chem. Soc.* **2005**, *127*, 3894−3909. (b) Evans, W. J.; Seibel, C. A.; Ziller, J. W. *Inorg. Chem.* **1998**, *37*, 770−776. (c) Evans, W. J.; Fujimoto, C. H.; Ziller, J. W. *Organometallics* **2001**, *20*, 4529−4536. (d) Evans, W. J.; Seibel, C. A.; Ziller, J. *Organometallics* **1998**, *17*, 2103-2112.

(24) (a) Blacque, O.; Brunner, H.; Kubicki, M. M.; Leblanc, J.-C.; Meier, W.; Moise, C.; Mugnier, Y.; Sadorge, A.; Wachter, J.; Zabel, M. *J. Organomet. Chem.* **2001**, *634*, 47−54. (b) Edwards, A. J.; Elipe, S.; Esteruelas, M. A.; Lahoz, F. J.; Oro, L. A.; Valero, C. *Organometallics* **1997**, *16*, 3828−3836. (c) Cuesta, L.; Gerbino, D. C.; Hevia, E.; Morales, D.; Clemente, M. E. N.; Pérez, J.; Riera, L.; Riera, V.; Miguel, D.; Rìo, I.; Garcìa-Granda, S. *Chem.—Eur. J.* **2004**, *10*, 1765−1777. (d) Ruiz, J.; Martinez, M. T.; Florenciano, F.; RodrIguez, V.; Lupez, G.; Pyrez, J.; Chaloner, P. A.; Hitchcock, P. B. *Inorg. Chem.* **2003**, *42*, 3650−3661.

Scheme 2

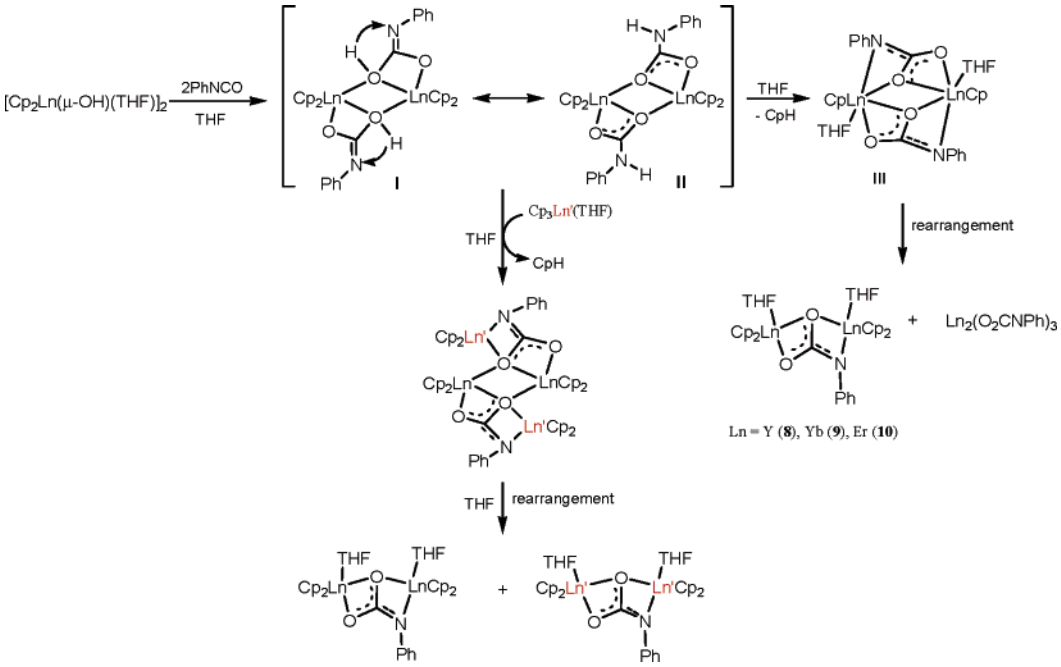

Scheme 3

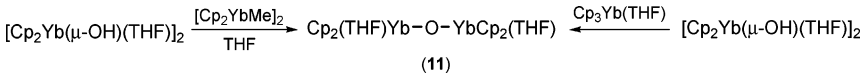

rapid reaction proceeds by hydrogen migration from oxonio to the C=C bond (Scheme 1). Presumably, the formation of a more-stable C−H bond compared with the N−H bond contributes to the different selectivity.

Although a wide variety of metal-promoted transformation reactions of isocyanates have been studied, few tandem reactions have been observed in the literature.[12,25,26] After having established that the newly formed carbaminate ligand is acidic enough to protonate the cyclopentadienyl ligand bound to the lanthanide center, we are interested in examining whether synthesis of heteronuclear organolanthanides was accessible by such a route. To that end, the reaction of $[Cp_2Y(\mu\text{-OH})(THF)]_2$ with PhNCO was immediately followed by adding Cp_3Yb; unfortunately, we isolated only rearrangement products $[Cp_2Y(THF)]_2(\mu\text{-}\eta^2\text{:}\eta^2\text{-}O_2CNPh)$ (**8**) and $[Cp_2Yb(THF)]_2(\mu\text{-}\eta^2\text{:}\eta^2\text{-}O_2CNPh)$ (**9**) rather than the expected heterodinuclear complex $(THF)Cp_2Yb(\mu\text{-}\eta^2\text{:}\eta^2\text{-}O_2CNPh)YCp_2(THF)$ (Scheme 2).

Reaction of $[Cp_2Ln(\mu\text{-OH})(THF)]_2$ with Cp_3Ln and with Lanthanocene Alkyls. Recently, $HC[CMeN(C_6H_3{}^iPr_2\text{-}2,6)]_2AlMe(OH)$ was found to allow the abstraction of one cyclopentadienyl ligand from Cp_3Ln, giving μ-oxo heterobimetallic oxides.[20] To obtain additional data on the organolanthanide hydroxide systems and to examine if organolanthanide hydroxides would undergo the analogous reaction, we also carried out the reaction of $[Cp_2Yb(\mu\text{-OH})(THF)]_2$ with Cp_3Yb. It was found that $[Cp_2Yb(\mu\text{-OH})(THF)]_2$ could slowly displace the cyclopentadienyl ligand of Cp_3Yb to give oxo-bridged complex $[Cp_2Yb(THF)]_2(\mu\text{-O})$ (**11**) (Scheme 3). Further study showed that complex **11** could be also obtained by reacting stoichiometric amounts of $[Cp_2Yb(\mu\text{-OH})(THF)]_2$ with $[Cp_2Yb(\mu\text{-Me})]_2$ at −30 °C. However, treatment of $[Cp_2ErCl]_2$ with Li^nBu followed by reaction with $[Cp_2Er(\mu\text{-OH})(THF)]_2$ affords μ-oxo lanthanocene cluster $(Cp_2Er)_3(\mu\text{-OH})(\mu_3\text{−O})(\mu\text{-Cl})Li(THF)_4$ (**12**) derived from partial hydrogen displacement of the OH ligands (Scheme 4). Presumably, the formation of **12** would be in part driven by the favorable stability at the expense of further reaction with the LiCl adduct of $Cp_2Ln^nBu(THF)_x$ or the mistaken stoichiometry. Further investigations on the formation pathway of **12** are currently in progress.

Scheme 4

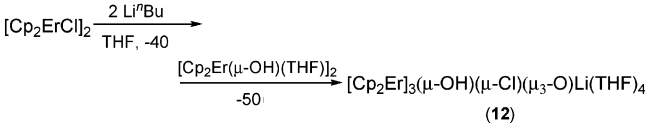

Complexes **4**−**12** are moderately sensitive to air and moisture; they dissolve in THF but are sparingly soluble in toluene and *n*-hexane. All complexes were characterized by element analysis and IR spectroscopies, the results of which are in good agreement with the proposed structures.

The IR spectra of **5**−**11** are devoid of O−H absorption in the range 3000−3500 cm^{-1}. For **5**−**7**, the presence of carboxylate was established by the observation of $\upsilon_{as}(CO_2^-)$ and $\upsilon_s(CO_2^-)$ at about 1570 and 1410 cm^{-1}, which correspond to the asymmetric vibrations of CO_2^- groups and symmetric stretches in metal-carboxylate complexes, respec-

(25) (a) Gambarotta, S.; Strologo, S.; Floriani, C.; Chiesi-Villa, A.; Guastini, C. *J. Am. Chem. Soc.* **1985**, *107*, 6278−6282.
(26) Tardif, O.; Hashizume, D.; Hou, Z. M. *J. Am. Chem. Soc.* **2004**, *126*, 8080−8181.

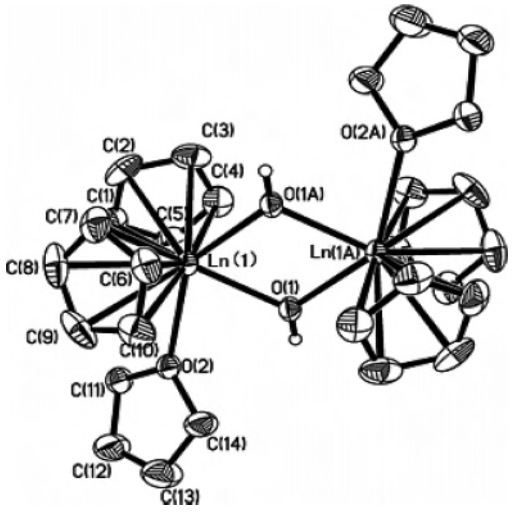

Figure 1. Molecular structure of $[Cp_2Ln(\mu\text{-OH})(THF)]_2$ (Ln = Y (**1**), Er (**2**)) (with 30% probability level thermal ellipsoids).

Table 4. Bond Lengths (Å) and Angles (deg) for Complexes **1** and **2**

	Ln = Y (**1**)	Ln = Er (**2**)
Ln(1)−O(1)	2.225(2)	2.224(4)
Ln(1)−O(1A)	2.257(2)	2.244(5)
Ln(1)−C(10)	2.663(4)	2.652(8)
Ln(1)−C(6)	2.685(4)	2.658(8)
Ln(1)−C(9)	2.693(4)	2.674(8)
Ln(1)−C(4)	2.700(4)	2.675(8)
Ln(1)−C(8)	2.701(4)	2.684(9)
Ln(1)−C(7)	2.702(4)	2.694(9)
Ln(1)−C(2)	2.703(4)	2.700(7)
Ln(1)−C(3)	2.705(4)	2.700(8)
Ln(1)−C(5)	2.711(4)	2.707(9)
Ln(1)−C(1)	2.717(4)	2.652(8)
Ln(1)−O(2)	2.533(2)	2.524(5)
O(1)−Ln (1)−O(1 A)	68.28(11)	68.60(19)
Ln (1)−O(1)−Ln (1A)	111.72(11)	111.40(19)

tively.[27] In the case of **8**−**10**, the IR exhibits, in addition to the characteristic absorption assigned to Cp and CO_2^- groups, two well-defined bands at about 1584 and 1051 cm^{-1} for phenyl and coordinated THF, respectively. The mass spectra of **5**−**7** display a series of peaks representing fragments derived from the parent molecules. Complex **8** has a ^1H NMR spectrum containing peaks consistent with Ph (7.16), C_5H_5 (6.49 and 6.30), and THF (3.57 and 1.42) and lacks the resonance of the NH proton.

Structural Description. Complexes **1** and **2** crystallize from the solvent THF in the monoclinic system, space group *P*2(1)/*c*. An ORTEP diagram of **1** and **2** is shown in Figure 1, and their selected bond distances and angles are given in Table 4. The structural data show that complexes **1** and **2** are centrosymmetric dimers. For complex **1**, The Y(1)−O(1)−Y(1A)−O(1A) bridging unit is coplanar. The mean bond distance of Y−O, 2.241(2) Å, is comparable to the corresponding Y−O distance of 2.202(2) Å in $[O(CH_2CH_2C_5H_4)_2Ln]_2(\mu\text{-PzMe})(\mu\text{-OH})$[14b] but is shorter than the 2.34(2) Å distance in $[Cp_2Y(\mu\text{-OH})]_2(PhCCPh)$.[14a] The O(1)−Y(1)−O(1A) angle of 68.28(11)° is smaller than the 80.3(9)° angle found in $[Cp_2Y(\mu\text{-OH})]_2(PhCCPh)$.[14a] The

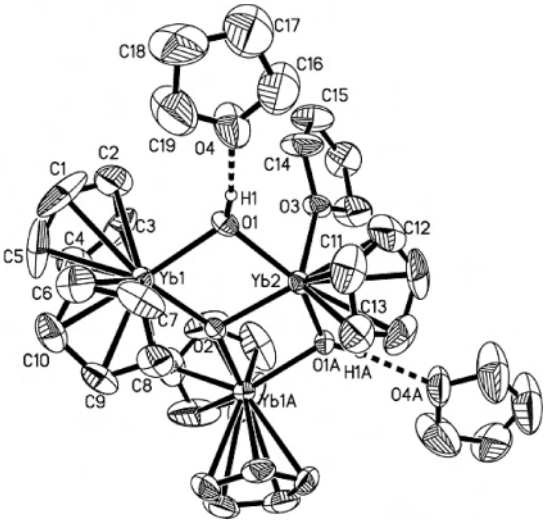

Figure 2. Molecular structure of $[Cp_2Yb(\mu\text{-OH})]_2[CpYb(THF)](\mu_3\text{-O})$ (**4**·2THF) (with 30% probability level thermal ellipsoids).

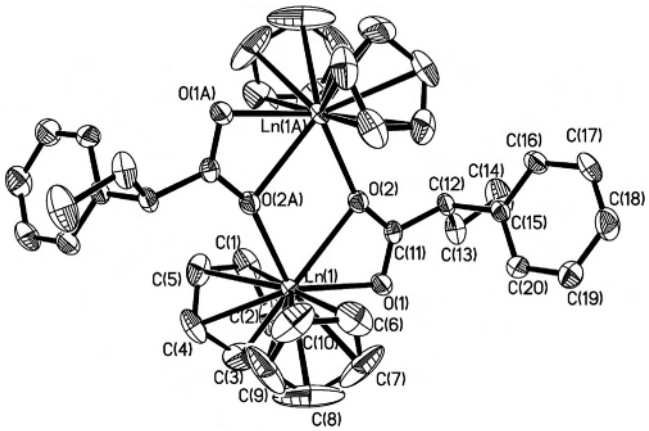

Figure 3. Molecular structure of $[Cp_2Ln(\mu\text{-}\eta^1\text{:}\eta^2\text{-}O_2CCHEtPh)]_2$ (Ln = Yb (**5**), Er (**6**), Y (**7**)) (with 30% probability level thermal ellipsoids).

structural parameters of **2** are very similar to those found in complex **1**. The average bond distance of Er−O (bridging OH) (2.234(4) Å) is nearly identical to the corresponding value of 2.237(2) Å in $[(CH_3OCH_2CH_2C_5H_4)_2Er(\mu\text{-OH})]_2$.[14d]

The structure of **4** is shown in Figure 2, and selected bond distances and angles are given in Table 5. The three Yb atoms are located in two different coordinate environments. Yb(1) and Yb(1A) are coordinated by two η^5-C_5H_5 groups and two bridging oxygen atoms, respectively, to form a distorted tetrahedron, whereas Yb(2) is coordinated to one η^5-C_5H_5, two oxygen atoms from bridging hydroxide ligands, one μ_3-O atom, and one THF oxygen atom, leading to a distorted trigonal-bipyramidal geometry. The Yb−O(μ_3-oxide) distances of 2.1173(18)−2.157(6) are longer than that observed for the μ-oxide group in $[(C_5H_4Me)_2Yb(THF)]_2(\mu\text{-O})$ (2.02 Å)[28] but shorter than the Yb−O(μ_4-oxide) distance in $(C_5H_4Me)_3Yb_4(\mu\text{-Cl})(\mu_3\text{-Cl})(\mu_4\text{-O})(THF)_3$ (2.28−2.29 Å).[29] The average Yb−O(μ-OH) length of 2.169 Å is shorter than that observed in $[(\eta^5\text{-}C_5H_4SiMe_3)_2Yb(\mu\text{-OH})]_2$.[14c] In addition, the

(27) Deacon, G. B.; Fallon, G. D.; Gatehouse, B. M.; Rabinovich, A.; Skelton, B. W.; White, A. H. *J. Organomet. Chem.* **1995**, *501*, 23−30.

(28) Adam, M.; Massarweh, G.; Fischer, R. D. *J. Organomet. Chem.* **1991**, *405*, C33−C37.

(29) Zhou, X. G.; Ma, H. Z.; Wu, Z. Z.; You, X. Z.; Xu, Z.; Huang, X. Y. *J. Organomet. Chem.* **1995**, *503*, 11−13.

Table 5. Bond Lengths (Å) and Angles (deg) for Complex **4**

Yb(1)−O(2)	2.1173(18)	Yb(1)−C(7)	2.636(11)
Yb(1)−O(1)	2.157(6)	Yb(2)−O(2)	2.156(7)
Yb(1)−C(9)	2.599(11)	Yb(2)−O(1)	2.180(7)
Yb(1)−C(1)	2.605(18)	Yb(2)−O(3)	2.277(8)
Yb(1)−C(4)	2.605(14)	Yb(2)−C(13)	2.604(18)
Yb(1)−C(2)	2.608(16)	Yb(2)−C(11A)	2.615(12)
Yb(1)−C(3)	2.614(12)	Yb(2)−C(11)	2.615(12)
Yb(1)−C(5)	2.616(16)	Yb(2)−C(12A)	2.622(11)
Yb(1)−C(8)	2.620(10)	Yb(2)−C(12)	2.622(11)
Yb(1)−C(6)	2.622(12)	O(1)−H(1)	0.845(10)
Yb(1)−C(10)	2.622(12)	H(1)···O(4)	2.031(18)
O(2)−Yb(1)−O(1)	77.1(2)	Yb(1)−O(1)−Yb(2)	101.4(2)
O(2)−Yb(2)−O(1A)	75.78(15)	Yb(1)−O(2)−Yb(1A)	151.0(4)
O(1)−Yb(2)−O(1A)	146.8(3)	Yb(1)−O(2)−Yb(2)	104.30(18)
Yb(1)−Yb(1A)−O(1A)	91.408	O(1A)−O(1)−Yb(1)	88.592
Yb(1A)−O(1A)−O(1)	88.592	O(1)−Yb(1)−Yb(1A)	91.408
O(1)−H(1)···O(4)	171(7)		

Table 6. Bond Lengths (Å) and Angles (deg) for Complex **5**−**7**

	Ln = Yb (**5**)	Ln = Er (**6**)	Ln = Y (**7**)
Ln(1)−O(2A)	2.265(5)	2.295(3)	2.316(4)
Ln(1)−O(1)	2.342(6)	2.371(3)	2.388(4)
Ln(1)−O(2)	2.435(5)	2.475(3)	2.486(4)
O(1)−C(11)	1.243(9)	1.237(5)	1.245(7)
O(2)−C(11)	1.274(9)	1.282(5)	1.286(7)
C(11)−C(12)	1.507(10)	1.506(6)	1.507(8)
Ln−C_{av}(Cp)	2.568(11)	2.602(7)	2.624(9)
O(2A)−Ln(1)−O(1)	120.9 (18)	120.6(11)	120.5(14)
O(2A)−Ln(1)−O(2)	67.4(2)	67.8(12)	67.8(15)
O(1)−Ln(1)−O(2)	53.7(17)	52.90(10)	52.8(13)
O(1)−C(11)−O(2)	118.0(6)	118.1(4)	118.1(5)
O(1)−C(11)−C(12)	121.2(7)	121.6(4)	121.2(6)
Ln(1A)−O(2)−Ln(1)	112.6(2)	112.2(12)	112.2(15)
O(2)−C(11)−Ln(1)	61.2(4)	61.5(2)	61.3(3)
O(1)−C(11)−Ln(1)	56.8(4)	56.6(2)	56.8(3)
O(2)−C(11)−C(12)	120.8(7)	120.3(4)	120.7(5)

Yb−O(THF) distance of 2.277(8) Å falls within the normal range of 2.25−2.40 Å.[30] Characteristically, O−H···O hydrogen bonding between the bridging OH group and the noncoordinated THF molecule is observed in **4**. The hydrogen-bond interaction is common in inorganic complexes of rare earth metals. For the lanthanocene hydroxide system, however, a similar interaction has not been observed previously. Seemingly, this feature may explain the fact that the solubility of **4** in THF is much larger than those of **1**−**3**.

X-ray analysis shows that complexes **5**−**7** are isomorphous and that each of them is a centrosymmetric dimeric structure (Figure 3) in which each the carboxylate ligand acts as both a bridging and side-on chelating group, forming three interlaced four-membered ring with Ln atoms. Each Ln atom is coordinated by two η^5-cyclopentadienyl groups, one chelating $O_2CCHEtPh$ ligand, and one bridging oxygen atom from another $O_2CCHEtPh$ moiety, such that the Ln atom has a coordination number of nine.

Important bond parameters of complexes **5**−**7** are listed in Table 6. In **5**, the 1.243(9) Å O(1)−C(11) and 1.274(9) Å O(2)−C(11) distances are between the 1.293−1.407 Å range of C(sp^2)−O and the 1.192−1.256 Å range of C(sp^2)═O distances.[31] The bond angles around C(11) are consistent with sp^2 hybridization. This suggests some electronic delocalization over OCO unit. The distance of C(11)−C(12), 1.507(10) Å, corresponds well to that of the C−C single bond. The chelation of **5** is quite unsymmetrical, with the difference being close to 0.1 Å between the Yb(1)−O(1) (2.342(6) Å) and Yb(1)−O(2) (2.435(5) Å) lengths, whereas in $[Cp_2Yb(\mu\text{-}O_2CMe)]_2$,[27] chelation is symmetrical. This suggests that the nature of substituents on the bridging carboxylate ligand affects the coordination geometry around the metal in the same way. The 2.265 Å Yb(1)−O(2A) distance is much shorter than the Yb(1)−O(1) (2.342(6) Å) and Yb(1)−O(2) (2.435(5) Å) bonds; the latter fall in the 2.30(1)−2.50(1) Å range of $Yb^{3+}\leftarrow{:}OR_2$ donating bond lengths for neutral oxygen-donor ligands.[32] These Yb−O distances are compared, respectively, to the corresponding distances in $[(C_5H_4PPh_2)_2Yb(\mu\text{-}O_2CMe)]_2$, 2.282(4), 2.3394(4), and 2.454(4) Å.[27]

All bond parameters for **6** and **7** are in normal ranges (Table 6), indicating that the hydroxide ligand is transformed to the carboxylate ligand via a formal insertion of ethylphenylketene into the O−H bond. Both complexes are dimeric with two carboxylate bridges, in which each carboxylate is chelated to one lanthanide ion and bridged through one oxygen atom to the other. The two C−O bond lengths in each structure are also indistinguishable and are nearly equal in the two structures, as are the O−C−O angles. The bond distances involving the metal in **6** and **7** are similar to the corresponding values in **5**, if the difference in metal radii is considered.[33]

The molecular structure of complexes **8**−**10** is shown in Figure 4, and selected bond distance and angles for each compound are listed in Table 7. For comparison purposes, a common atomic numbering scheme has been used. All three complexes are solvated O_2CNPh-bridged binuclear structures. One Ln atom is nine-coordinated by two η^5-cyclopentadienyl groups, one coordinated THF, and two oxygen atoms of the O_2CNPh ligand, whereas another Ln atom is coordinated by two η^5-cyclopentadienyl groups, two oxygen atoms from coordinated THF and the O_2CNPh bridge, respectively, and

(30) (a) Adem, M.; Li, X. F.; Oroschin, W.; Fischer, R. D. *J. Organomet. Chem.* **1985**, *296*, C19−C22. (b) Qian, C.; Wang, B.; Deng, D.; Xu, C.; Sun, X.; Ling, R. *Chin. J. Struct.* **1993**, *12*, 18−21.
(31) Allen, F. H.; Kennard, O.; Watson, D. G.; Brammer, L.; Orpen, A. G. *J. Chem. Soc., Perkin Trans.* **1987**, S1−S19.
(32) (a) Willey, G. R.; Woodman, T. J.; Errington, W. *J. Indian Chem. Soc.* **1998**, *75*, 435−438. (b) Cheung, M.-S.; Chan, H.-S.; Xie, Z. W. *Organometallics* **2005**, *24*, 4468−4474.
(33) Shannon, R. D. *Acta Crystallogr., Sect. A* **1976**, *32*, 751−767.

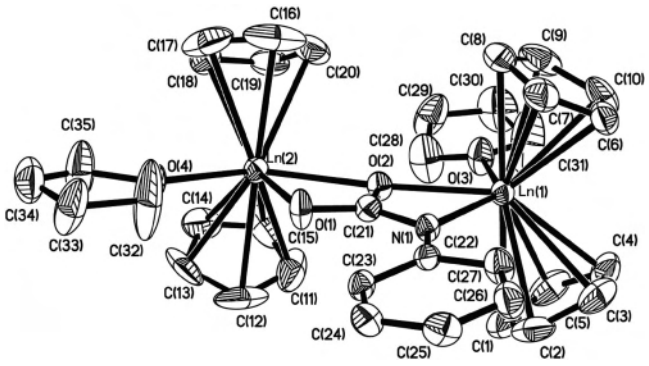

Figure 4. Molecular structure of $[Cp_2Ln(THF)]_2(\mu\text{-}\eta^2\text{:}\eta^2\text{-}O_2CNPh)$ (Ln = Y (**8**), Yb (**9**), Er (**10**)) (with 30% probability level thermal ellipsoids).

Table 7. Bond Lengths (Å) and Angles (deg) for Complex **8**−**10**

	Ln = Y (**8**)	Ln = Yb (**9**)	Ln = Er (**10**)
Ln(1)−O(2)	2.356(4)	2.319(6)	2.348(3)
Ln(1)−N(1)	2.367(5)	2.369(7)	2.370(3)
Ln(1)−O(3)	2.446(4)	2.437(7)	2.452(3)
Ln−C_{av}(Cp)	2.654(8)	2.617(13)	2.643(6)
N(1)−C(21)	1.313(6)	1.312(11)	1.314(5)
Ln(2)−O(1)	2.269(4)	2.220(6)	2.252(3)
Ln(2)−O(4)	2.391(4)	2.389(7)	2.396(3)
Ln(2)−O(2)	2.440(4)	2.445(6)	2.439(3)
O(1)−C(21)	1.293(6)	1.276(11)	1.279(5)
O(2)−C(21)	1.328(6)	1.324(10)	1.333(5)
O(2)−Ln(1)−N(1)	56.3(13)	56.9(2)	56.43(11)
O(1)−Ln(2)−O(2)	56.0(14)	56.0(2)	56.0 (10)
O(1)−C(21)−N(1)	129.6(6)	128.5(9)	129.5(4)
O(1)−C(21)−O(2)	115.4(5)	115.7(8)	115.6(4)
C(21)−N(1)−Ln(1)	94.2(4)	92.6(5)	94.1(3)
C(21)−O(1)−Ln(2)	98.7(4)	100.0(5)	99.2(3)
C(21)−O(2)−Ln(1)	94.3(3)	94.5(5)	94.5(2)
C(21)−O(2)−Ln(2)	89.9(3)	88.3(5)	89.1(2)
Ln(1)−O(2)−Ln(2)	174.9(17)	175.8(3)	175.4(13)
N(1)−C(21)−O(2)	115.0(6)	115.9(8)	114.9(4)

one N atom of the O_2CNPh unit; its formal coordination number is nine.

The bond lengths of O(1)−C(21) and O(2)−C(21) in **8**, 1.293(6) and 1.328(6) Å, respectively, are between the lengths of the C(sp^2)═O double bond and C(sp^2)−O single bond;[31] further, the C(21)−N(1) distance of 1.313(6) Å also lies between the typical 1.279−1.329 Å C(sp^2)═N distance and 1.321−1.416 Å range of the C(sp^2)−N bond,[23c] and the O_2CN core is planar with the sum of its angles being 360°. These results indicate the delocalization of negative charge over the O_2CN unit. The 2.367(5) Å Y(1)−N(1) distance is similar to that found in $(C_5Me_5)_2Y[N(SiMe_3)_2]$ (2.324(7) Å)[34] and $(C_5Me_4Et)_2Y[N(SiMe_3)_2]$ (2.39(1) Å)[35] but shorter than the Y←:N donor bond distances in complexes $(C_5H_5)_2Y[C_6H_4(o\text{-}CH_2NMe_2)]$[36] and $(C_5Me_5)Y[C_6H_4(o\text{-}CH_2NMe_2)]_2$,[37] which range from 2.43(2) to 2.588(5) Å. The average value of Y−C(Cp) distances, 2.654 Å, is in the normal range for

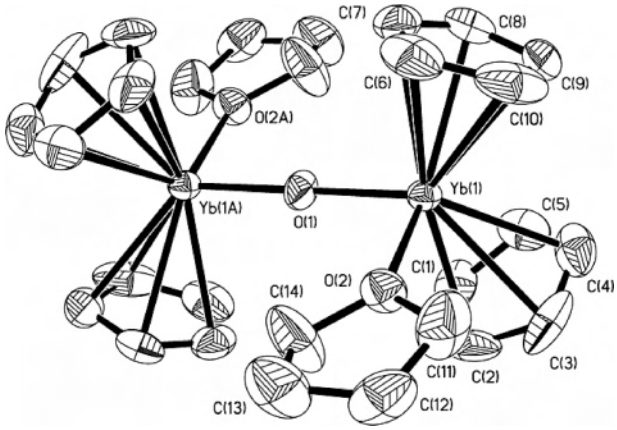

Figure 5. Molecular structure of $[Cp_2Yb(THF)]_2(\mu\text{-O})$ (**11**) (with 30% probability level thermal ellipsoids).

Table 8. Bond Lengths (Å) and Angles (deg) for Complex **11**

Yb(1)−O(1)	2.004(7)	O(1)−Yb(1A)	2.004(7)
Yb(1)−C(1)	2.604(8)	Yb(1)−C(5)	2.642(9)
Yb(1)−C(7)	2.614(8)	Yb(1)−C(10)	2.647(11)
Yb(1)−C(6)	2.623(10)	Yb(1)−C(9)	2.662(9)
Yb(1)−C(8)	2.625(8)	Yb(1)−C(4)	2.664(10)
Yb(1)−C(2)	2.626(9)	Yb(1)−C(3)	2.677(11)
Yb(1)−O(1)−Yb(1A)	180.00	O(1)−Yb(1)−O(2)	93.92(15)

yttrium metallocenes, such as $[(MeC_5H_4)_2Y(\mu\text{-}OCH{=}CH_2)]_2$ (2.651 Å).[38]

Complex **9** is isostructural to complex **8**. The Yb(1)−N(1) (2.369(7) Å) distance is similar to that in $[(C_5H_4Me)_2Yb(\mu\text{-}NC_6H_{10}O)]_2$, 2.374(4) Å.[39] The shorter Yb(2)−O(1) (2.220-(6) Å) and longer Yb(1)−O(2) (2.319(6) Å) distances (Table 7) compared to the corresponding ones in **5** indicate a stronger bonding interaction of the Yb and chelating O atoms in **9**. Furthermore, the O(1)−Yb(2)−O(2) angle of 56.0(2)° in **9** is slightly larger than the corresponding value of 53.7-(2)° in **5**.

The molecular structure of complex **11** is shown in Figure 5, and selected bond distance and angles are listed in Table 8. Each of lanthanide ions possesses a pseudotetrahedral geometry surrounded by two cyclopentadienyl rings and two oxygen atoms. The Yb(1)−O(1)−Yb(1A) angle of 180.0° in **11** is quite identical to the values observed in $[Cp_2Lu(THF)]_2(\mu\text{-O})$[40] and $[(Me_2C{=}CHC_5H_4)_2Y(Et_2O)]_2(\mu\text{-O})$[41] but significantly larger than those found in heterobimetallic oxides such as $Cp_2Yb(THF)OAlMe[HC(CMeNC_6H_3{}^iPr_2\text{-}2,6)_2]$ (169.5 °), $Cp_2YbOAlMe[HC(CMeNC_6H_3{}^iPr_2\text{-}2,6)_2]$ (168.8 °),[20] and $CH[CMeN(C_6H_3{}^iPr_2\text{-}2,6)]_2GeOM(Me)Cp_2$ (M = Zr, 143.8(1)°; M = Hf, 141.9(2)°).[42] The Yb−O distances in **11** are similar to the corresponding ones in $[(C_5H_4Me)_2Yb(THF)]_2(\mu\text{-O})$ (2.02 and 2.35 Å)[28] and $Cp_2Yb(THF)OAlMe[HC(CMeNC_6H_3{}^iPr_2\text{-}2,6)]$ (2.02 and 2.37 Å).[20]

(34) De Haan, K. H.; De Boer, J. L.; Teuben, J. H.; Spek, A. L.; Kojiæ-Prodiæ, B.; Hays, G. R.; Huis, R. *Organometallics* **1986**, *5*, 1726−1733.
(35) Schumann, H.; Rosenthal, E. C.; Kociok-Köhn, G.; Molander, G. A.; Winterfeld, J. *J. Organomet. Chem.* **1995**, *496*, 233−240.
(36) Rausch, M. D.; Foust, D. F.; Rogers, R. D.; Atwood, J. L. *J. Organomet. Chem.* **1984**, *3*, 241−248.
(37) Booij, M.; Kiers, N. H.; Meetsma, A.; Teuben, J. H. *Organometallics* **1989**, *8*, 2454−2461.
(38) Evans, W. J.; Dominguez, R.; Hanusa, T. P. *Organometallics* **1986**, *5*, 1291−1296.
(39) Shen, Q.; Wang, Y.; Wu, L.; Zhang, Y.; Sun, J. *J. Organomet. Chem.* **2001**, *626*, 176−180.
(40) Schumann, H.; Palamidis, E.; Loebel, J. *J. Organomet. Chem.* **1990**, *384*, C49−C52.
(41) Schumann, H.; Heim, A.; Demtschuk, J.; Mühle, S. H. *Organometallics* **2003**, *22*, 118−128.
(42) Pineda, L. W.; Jancik, V.; Roesky, H. W.; Herbst-Irmer, R. *Inorg. Chem.* **2005**, *44*, 3537−3540.

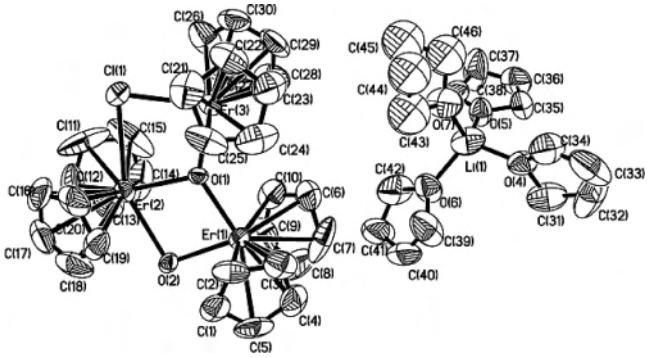

Figure 6. Molecular structure of $(Cp_2Er)_3(\mu\text{-OH})(\mu_3\text{-O})(\mu\text{-Cl})Li(THF)_4$ (**12**) (with 30% probability level thermal ellipsoids.

Table 9. Bond Lengths (Å) and Angles (deg) for Complex **12**

Er(1)−O(1)	2.167(6)	Er(2)−O(1)	2.228(7)
Er(1)−O(2)	2.380(7)	Er(2)−O(2)	2.521(7)
Er(3)−O(1)	2.130(6)	Li(1)−O(5)	1.84(4)
Er(3)−Cl(1)	2.580(4)	Li(1)−O(7)	1.87(3)
Er(2)−Cl(1)	2.944(4)	Li(1)−O(6)	1.95(4)
Er(1)−C_{av}(Cp)	2.666(13)	Li(1)−O(4)	1.97(4)
Er(3)−C_{av}(Cp)	2.644(15)	Er(2)−C_{av}(Cp)	2.650(17)
O(1)−Er(1)−O(2)	82.0(3)	Er(1)−O(1)−Er(2)	107.5(3)
O(1)−Er(2)−O(2)	77.7(2)	Er(1)−O(2)−Er(2)	92.6(3)

Complex **12** exists as discrete cation and anion pairs, each with no crystallographically imposed symmetry. Selected bond distance and angles are listed in Table 9. The anion shown in Figure 6 is comprised of three dicyclopentadienyl erbium units arranged in a triangular array. Two sides of the triangle are bridged by one hydroxide ligand and one chloride ion, respectively, and an additional μ_3-oxo resides in the interior of the triangle, which provides a formal coordination number of nine for Er(2) and eight for Er(1) and Er(3) atoms. The difference between Er(3)−Cl(1) (2.580(4) Å) and Er(2)−Cl(1) (2.944(4) Å) may be related to the position of the central oxygen atom. The latter is the longest Er−Cl(μ_2-bridging) separation observed thus far.[43] The parameters associated with the $Li(THF)^{4+}$ cation are normal.

(43) Wu, Z. Z.; Xu, Z.; You, X. Z.; Wang, H. Q.; Zhou, X. G. *Polyhedron* **1993**, *12*, 677−681.

Conclusion

In summary, we describe some new classes of reactions of lanthanocene hydroxides with heteroallenes and selected lanthanide precursors. The hydroxide group shows selective reactivity, and different types of lanthanocene derivatives containing carboxylate, carbaminate, or oxo-bridged ligands were obtained through O−H addition and/or hydrogen displacement of the OH ligand. This shows that the hydroxide ligand of the organolanthanide complexes is a potential proton acid that is capable of reacting with different heteroallene molecules and basic reagents under mild reaction conditions, allowing for regioselective introduction of a variety of alternate substituents such as acyl, carbamoyl, and the metal-containing moiety onto the oxygen atom. Thus, lanthanocene hydroxide complexes proved to be easily accessible for synthesis of lanthanocene derivatives in a manner consistent with a ligand-based reaction pattern. Noticeably, the insertion of an organic functional group into the heteroatom−hydrogen bond of organolanthanides remains little explored, despite the fact that such reactions are also of primary importance, as they lie at the basis of lanthanide-promoted functionalizations and may lead to new synthetic methodology and new organolanthanide derivatives. This work provides a new insight into the ligand-forming and transforming behavior of organolanthanides and exemplifies the potential of the OH ligand in further functionalization. Furthermore, the formation of **8**−**10** represents a unique reactivity of isocyanates toward organometallic complexes.

Acknowledgment. We thank the NNSF of China, the NSF of Shanghai, the Fund of the New Century Distinguished Scientist of the Education Ministry of China, and the Research Fund for the Doctoral Program of Higher Education of China for financial support.

Supporting Information Available: Tables of atomic coordinates and thermal parameters, all bond distances and angles, and experimental data for all structurally characterized complexes. This material is available free of charge via the Internet at http://pubs.acs.org.

IC0602998